ISSN 1330-3651 (Print), ISSN 1848-6339 (Online)
UDC/UDK 621.867.1:620.9

CONVEYOR DESIGN OPTIMIZATION AS THE PROVISION OF SUSTAINABILITY

Marko Langerholc, Nenad Zrnić, Miloš Đorđević, Boris Jerman

Original scientific paper
Conveyors are machines which typically operate continuously during long periods of time. Even a small increase in energy efficiency leads toward considerable energy savings and therefore improved sustainability. The energy is consumed to overcome dissipative effects and for possible lifting of transported goods. It can be saved only by reducing the dissipative effects. In the paper an example is introduced of two designs of the production machine chain conveyor. The effect of the changes of the design on the energy consumption is established. The dissipative effects are defined using analytical approach which is verified by means of measurements. Improved sustainability in the case of the second design is proven and discussed.

Keywords: *analytical approach, continuous operation, conveyors, efficiency, energy consumption, measurements, sustainability*

Optimiziranje konstrukcije konvejera kao uvjet održivosti

Izvorni znanstveni članak
Konvejeri su strojevi koji u principu rade neprekidno tijekom dugih vremenskih perioda. Čak i malo povećanje energetske učinkovitosti dovodi do znatnih ušteda energije, dakle do bolje održivosti. Energija se troši na svladavanje disipativnih učinaka i moguće podizanje transportiranih roba. Može se uštedjeti jedino smanjenjem disipativnih učinaka. U radu se daje primjer dviju konstrukcija lančanog konvejera proizvodnog stroja. Utvrđen je učinak promjena konstrukcije na potrošnju energije. Disipativni učinci definiraju se primjenom analitičkog pristupa verificiranog mjerenjima. Dokazana je i obrazložena poboljšana održivost u slučaju druge konstrukcije.

Ključne riječi: *analitički pristup, neprekinuti rad, konvejeri, učinkovitost, potrošnja energije, mjerenja, održivost*

1 Introduction

Although the conveyor systems are mostly used for transportation of goods in mines, depositories of bulk material, and through production lines, their specific usage inside production machines is also possible. For such tasks chain conveyors are frequently used. They can operate under heavy operating conditions like heavy loading, impacts, elevated temperatures, dust, etc.

There are number of ways to accomplish high level of sustainability of conveyor systems, which normally reduces overall operation costs too. Here the approach will be presented that assumes accomplishing of high level of sustainability through choosing an appropriate design of chain conveyor system. Another approach related to the utilisation of energetically optimised drives will be described later in this chapter.

Concept of sustainability can be interpreted differently depending on the point of view. From the environmental point of view, sustainability represents the system's capacity (in this case the Earth) to support mankind activities' impact upon the environment without putting under risk the future of human race. From the designer point of view, sustainable development is about designing objects that use limited resources; it is also about social responsibility and ethics. According to the future challenges for the intralogistics sector with respect to megatrends presented in [1] the focus of the current and forthcoming researches will be sustainability and energy efficiency of material handling and conveying equipment, technologies and systems.

Many verified designs exist for different types of conveying systems, corresponding to appointed applications, [2] but because of different specific operating conditions or because of potential cost reduction, engineers often have to search for new conveyor designs. For these solutions a required drive power is to be predicted in advance to enable an effective design process. Disregarding this request can cause high operational costs or costs of redesigning the finished machine.

Drive power estimation begins by identifying external loads acting on the conveyor. The process is continued with assessment of dissipative effects and determination of the required torque and power of chosen actuators, [3 ÷ 5]. Finally, the load bearing and other essential elements are designed or chosen accordingly.

The dissipative effects consist mainly of friction between parts in relative motion and depend on the type of friction, type and degree of lubrication and loading. The loading originates from conveyor weight, transported material weight, chain straining forces, possible production forces (if conveyor is in the production machine) and other design conditions.

Even when operating conditions are well known, the exact values of friction factor are hard to define. When operating conditions are hardly known because of, for instance, high and uneven operating temperature, manufacturing and assembling irregularities, uneven transported material distribution, poorly defined production forces, and unsteady lubrication, the friction determination becomes more difficult. In such cases more rough estimation of the dissipative effects during design is permissible and it should be followed by the measurements on the manufactured conveyor system.

After determination of the dissipative effects the ways for their reduction can be considered. Reduction of these dissipative effects results in improved energy efficiency and also in cost reduction.

Energy efficiency means using less energy inputs while maintaining an equivalent level of economic activity or service, [6, 7]. Energy saving is a broader concept that also includes consumption reduction through behaviour change or decreased economic activity [6, 7]. Energy efficient equipment becomes more attractive also from the economic point of view [8].

According to a publication of the German Federal Environmental Agency, the industrial electric power consumption is caused to more than 60 % by electric motors (see Fig. 1). Process heat, lightening or heating use proportionately less power, but should not remain unconsidered when talking about energy efficiency [8].

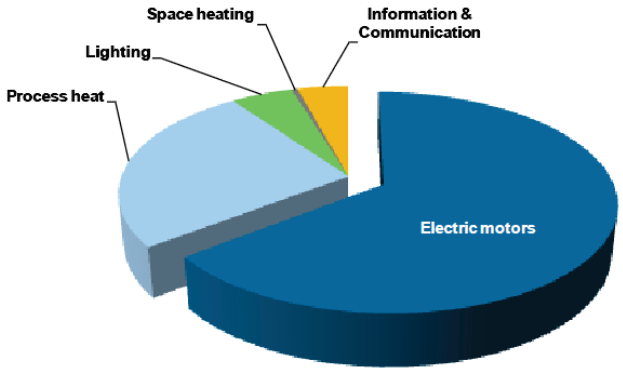

Figure 1 Electric power consumption in the German industry

The Bavarian Environment Agency clearly showed by the following number that energy efficient systems play an important role. If someone uses an electric motor with an annual service life of more than 3000 hours, 95 % of the entire costs during the durability fall upon energy consumption, less than 3 % upon acquisition. It is therefore too short-sighted to make a decision only dependent on the acquisition price, as just the energy consumption of electric drives can be optimized, e.g., in using frequency controlled efficient motors, low-loss transmission-units and an intelligent control. Savings of up to 40 % are possible here. It is important to consider the interaction of the entire conveyor chain, besides the individual conveyor elements. Capable conveyor lines fulfil many transport tasks more quickly, which can lead to a reduced runtime of the machines and therefore to a reduced consumption. Another possibility to reduce the energy consumption is to use energy optimized components [9].

Herman and Thiede simulated energy efficiency of the complete process chain. They pointed out the importance of considering the interdependency of all technical processes and of using an appropriate simulation approach [10].

Duflou et al. [11] use a structured approach, (distinguishing different system scale levels, starting from a unit process focus, the multi-machine, factory, multi-facility and also supply chain levels) in order to provide a systematic overview of the state of the art in energy and resource efficiency increasing methods and techniques.

This paper deals with the first mentioned approach for achieving high level of sustainability by appropriate design solution using unit process focus. Here are introduced and analysed two designs of a special chain conveyor system for production machine. Comparison of power dissipation in both cases shows essential improvement in the case of the second design.

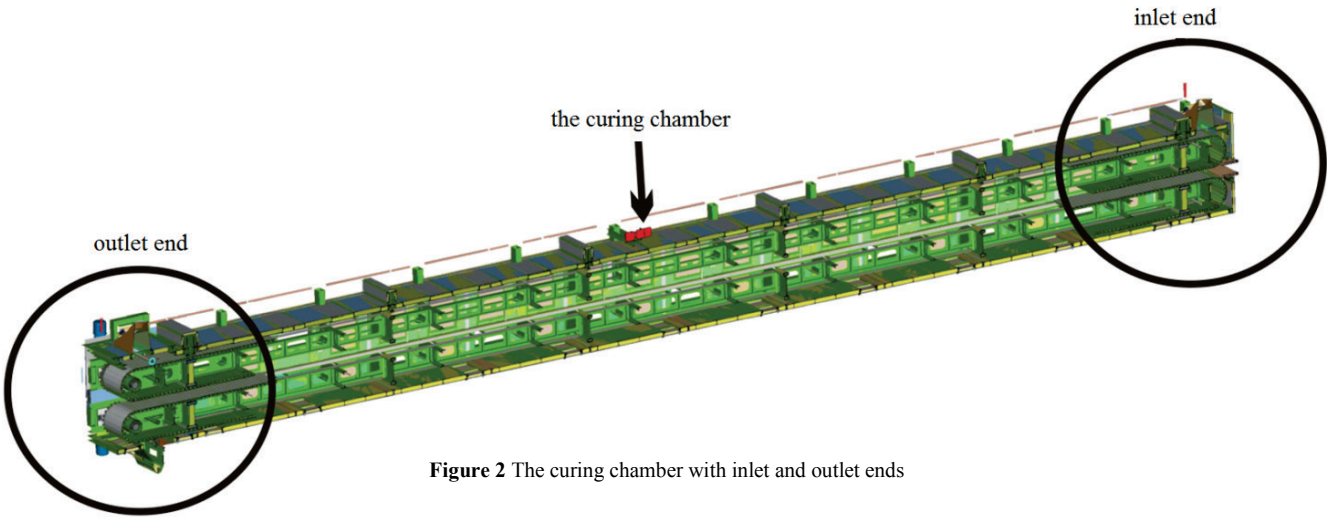

Figure 2 The curing chamber with inlet and outlet ends

2 Conveyor design solutions

Conveyor systems are important components of production lines, such as chambers for production of sandwich panels and curing chambers for production of mineral wool insulation plates.

The latter are used to achieve the required density, thickness and shape of insulation plates within the prescribed tolerances. To enable binding of separate mineral fibres into compact insulation plate the elevated temperature with average around 250 °C is needed in order to activate the present glue. The process of binder consolidation is realised by dehumidification in the curing chamber. For this reason a chain conveyor with perforated transverse girders is used, enabling sufficient air flow through the mineral fibres.

Fig. 2 shows the curing chamber with engaged chain conveyor system. The upper and lower chain conveyors are shown, stretching from the inlet to the outlet end of the chamber.

The details of the outlet and inlet ends of the curing chamber are shown in Figs. 3 and 4 respectively where also the chain conveyors with perforated transverse girders can be seen.

These conveyors are designed each with two pulling chains located on both sides of the conveyor belt and with two supporting chains located a quarter of the belt width

from the sides of the belt as shown in Fig. 5. All supporting and pulling chains are lubricated.

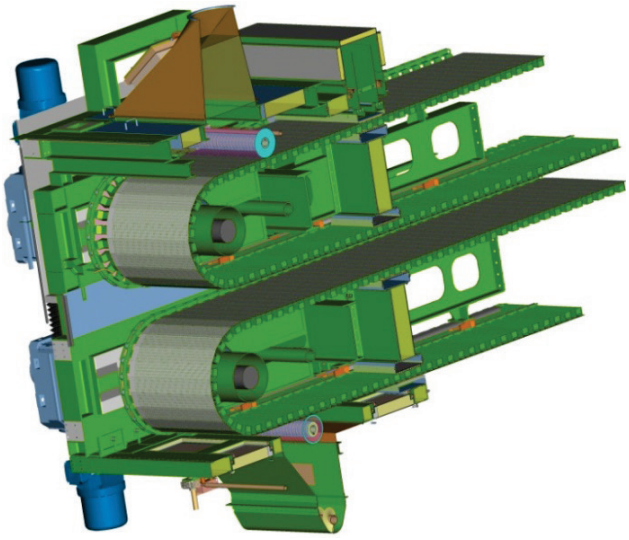

Figure 3 The outlet end of the curing chamber (the same for the basic and improved design)

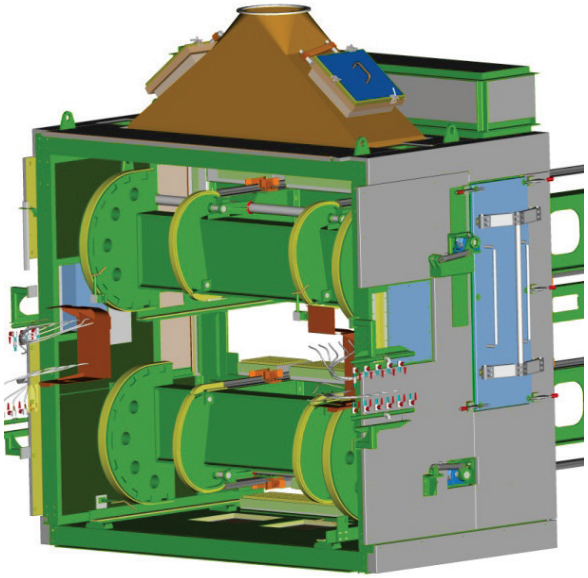

Figure 4 The inlet end of the curing chamber of the basic design

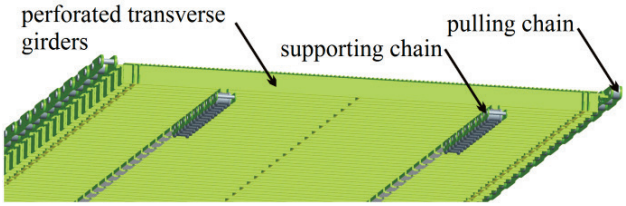

Figure 5 The conveyor belt made of perforated transverse girders with pulling chains and supporting chains

In the outlet end of the curing chamber the chain conveyors have rather conventional design of belt turn. Two sprocket-wheels are mounted on a driving shaft to transfer the driving moment of the electric motors to the pulling chains. The outlet end belt turn stays unchanged in both analysed cases.

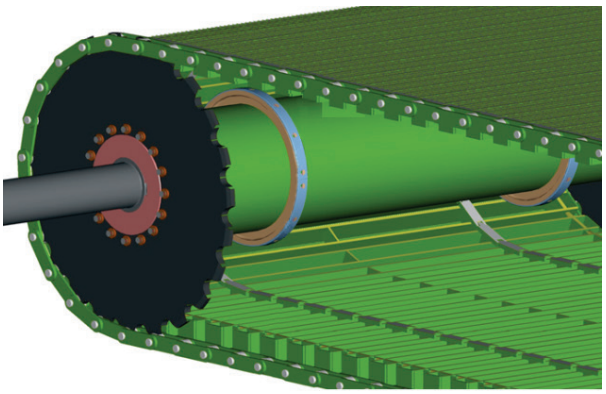

Figure 6 Close-up detail of driving shaft with sprocket-wheel

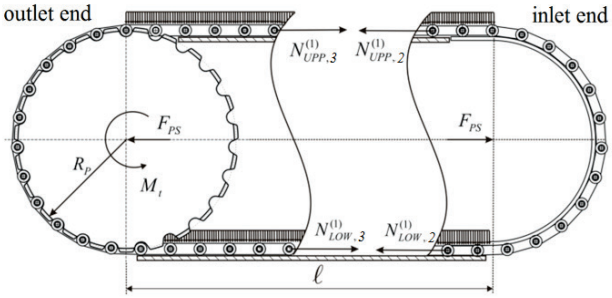

Figure 8 The basic design of pulling chain turns

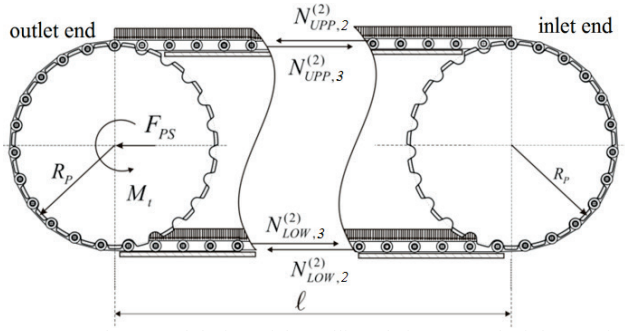

Figure 9 The second design of the pulling chain turns – the inlet turn is changed

On the other hand the inlet end of the conveyor belt turn deviates from the classic design solutions. Instead of the rotating shaft with wheels the fixed curved rolling surfaces are introduced for guidance of all of the chains. Such a design is simpler and cheaper to produce, but on the other hand the chains rollers are employed to enable the motion. As is proven later in the paper this solution is producing additional friction losses. The described configuration for one pulling chain is shown in Fig. 8.

For the reason of avoiding additional substantial energy dissipation the chain conveyor's turn at the inlet end was redesigned. The classic solution with the shaft was employed in the second design reducing the need of the chain rollers rotation at the belt turn to the minimum and transferring the relative motion from the chain rollers to the shaft bearings. This brought up an essential improvement of the efficiency. The described configuration for one pulling chain is shown in Fig. 9.

3 The measurements

The power, necessary for driving the lower chain conveyor was determined for both described conveyor

designs by means of measurement of the electric voltage, electric current and rotational velocity of the driving three phase squirrel cage electric motors and the following equation:

$$P_{\mathrm{D}}^{\mathrm{Ex}} = \omega_{\mathrm{M}} \cdot M_{\mathrm{M}} = 2\pi \cdot M_{\mathrm{M}} \cdot n_{\mathrm{M}} = M_{\mathrm{M}} \cdot \frac{v \cdot i}{R_{\mathrm{P}}}, \quad (1)$$

where i stands for drive gear ratio and motor moment M_{M} is calculated from basic quantities as:

$$M_{\mathrm{M}} = M_{\mathrm{N}} \cdot \frac{\sqrt{\left(\frac{I}{I_{\mathrm{N}}}\right) - (1 - \cos^2\varphi_{\mathrm{N}})}}{\cos\varphi_{\mathrm{N}}}, \quad (2)$$

where M_{N}, I_{N} and $\cos\varphi_{\mathrm{N}}$ are driving motor nominal electric quantities and I is an actual motor current.

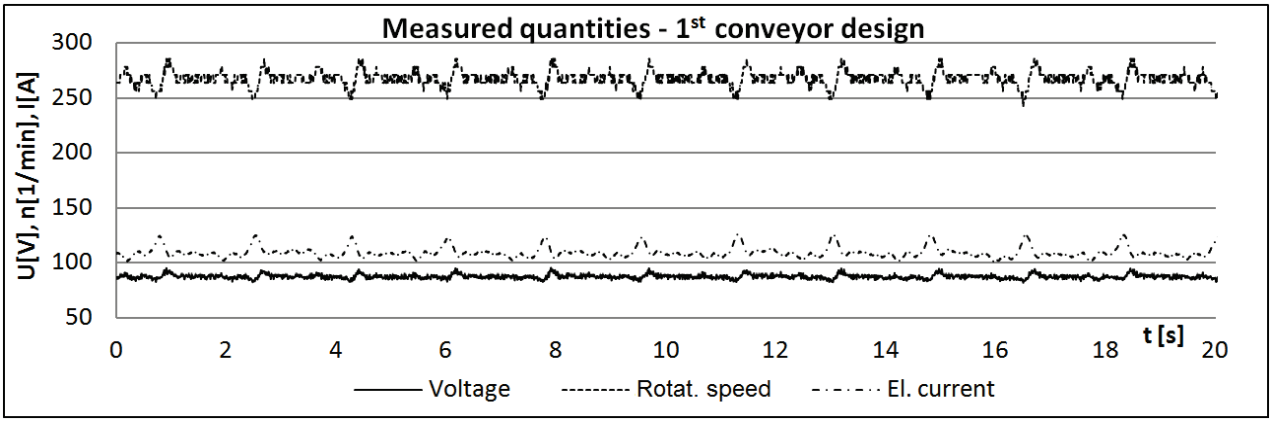

Figure 10 Measurements of voltage, el. current and rotational velocity of the driving motor of basic conveyor design

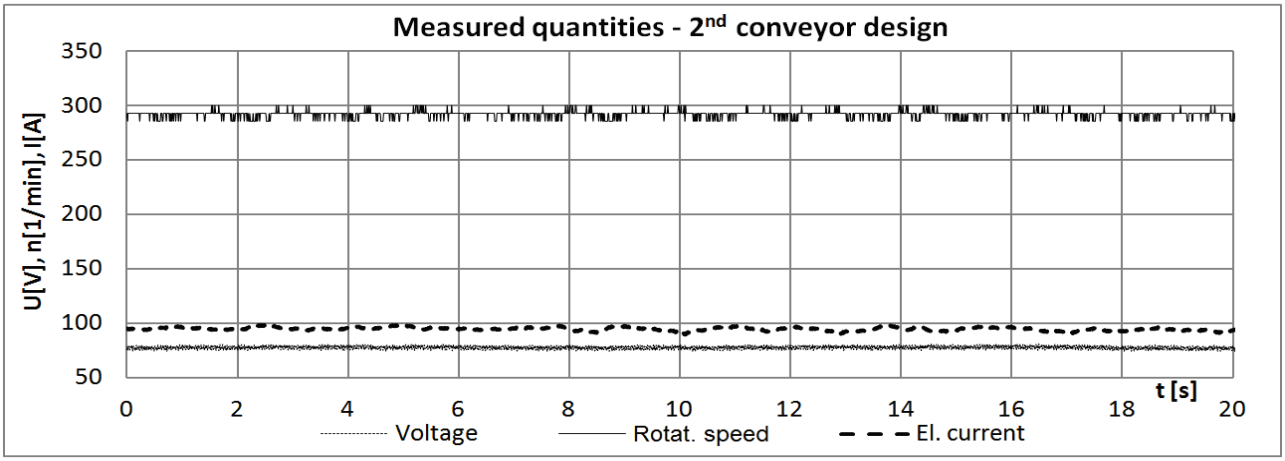

Figure 11 Measurements of voltage, el. current and rotational velocity of the driving motor of improved conveyor design

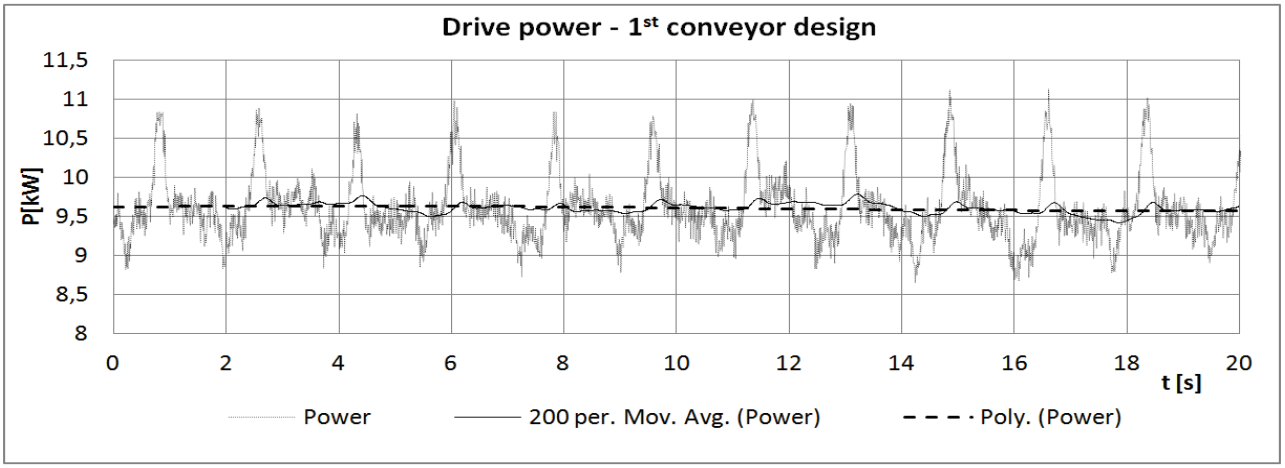

Figure 12 Drive power of the driving motor of basic conveyor design

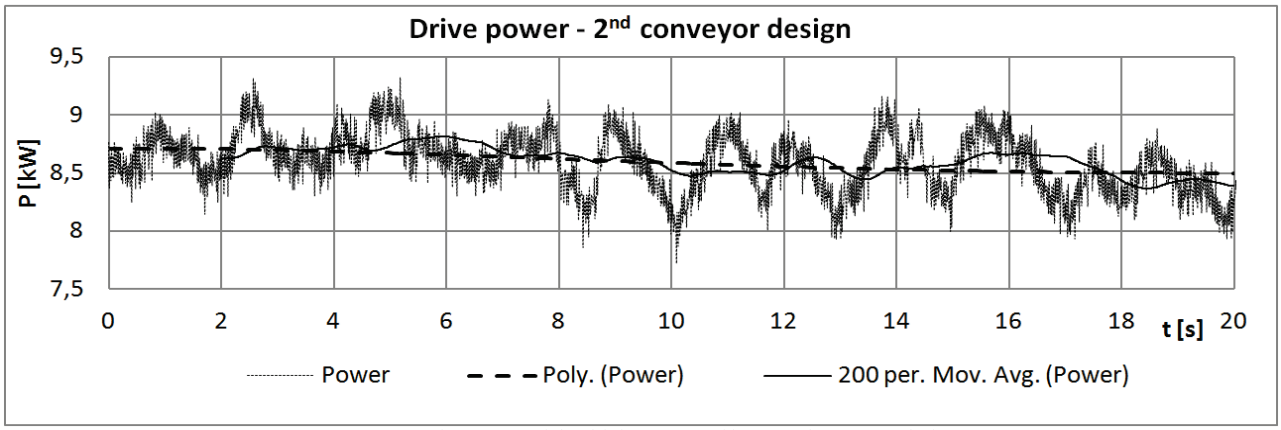

Figure 13 Drive power of the driving motor of improved conveyor design

The results of measurements and the diagrams of the required power are shown in Figs. 10 ÷ 13. It is clear from Figs. 10 and 11 that electric current and voltage have lower values in the case of the second design in comparison to the basic design whereas the achieved rotational velocity of the motor is greater. That all points to the lower energy dissipation and therefore to the improved efficiency of the conveyor system.

Electric power required for driving the lower chain conveyor, calculated from the measured quantities, is shown in Figs. 12 and 13. Average power decreased from 9,6 kW for the basic design to 8,7 kW for the changed design resulting in 9,0 % lower power consumption.

Additional observation showed that power curve had lower values and fluctuations. Power level fluctuations decreased from 2,3 kW (24 % of an average power) to 1,5 kW (17 % of an average power).

The power peaks that denote oncoming chain links were much lower indicating smoother operation of the conveyor which provides its longer life span and more constant production parameters.

Besides the basic curve that shows power consumption, there are two regression curves shown in Figs. 12 and 13. The bold continuous line presents regression curve of the Moving Average type with period of 200, and the dashed line of the Polynomial type.

4 Analytical approach

Measurements show that the basic (from some points of view fresh and innovative) design is not appropriate because of bigger energy consumption. The question is raised in this chapter whether the precise enough prediction of energy dissipation can be made in advance, using recognised analytical methods and known approximations of input variables, to make a relevant comparison of both designs regarding energy consumption and preventing the manufacturer from additional costs for changes of real world conveyor structure.

First of all the chain manufacturer's method for determination of the energy losses was examined. It was estimated that this method cannot be employed in the observed case, because the chain turn without sprocket wheel cannot be taken into account.

For this reason for the analysis the theoretical approach is employed. Friction model is established through evaluation of different friction contributions which are then combined to denote an overall conveyor movement resistance. It is presumed that the support chains are used to carry all normal loads along the length of the conveyor and that all axial forces are carried by pulling chains. The rolling and sliding friction types are included in the general friction model:

$$F_{\mathrm{f}} = F_{\mathrm{rf}} + F_{\mathrm{sf}} = \frac{f}{r} \cdot F'_{\mathrm{N}} + \mu \cdot F''_{\mathrm{N}}, \tag{3}$$

where F_{rf} and F_{sf} are rolling and sliding friction resistances, f is rolling resistance coefficient, r is chain roller radius, μ is coefficient of sliding friction, F'_{N} and F''_{N} are corresponding normal loads.

Coefficients f and μ depend mostly on materials in contact, on lubrication, and on working temperature. The temperature and lubrication influence is therefore considered through the appropriate friction coefficients.

4.1 The sources of the dissipative effects

The following sources of the dissipative effects are considered:

(1) The first source of friction contribution comes from the conveyor own weight, the integral weight of transported material, and from existing production forces, which acts perpendicular to the conveyor's surface and is distributed onto two supporting chains. The double roller contact is formed between the chain and both, the conveyor belt and the supporting track. The necessary drive moment to overcome this friction is:

$$M_{\mathrm{fl}} = R_{\mathrm{P}} \cdot F_{\mathrm{fl}}(T, \mathrm{lub}), \tag{4}$$

where $F_{\mathrm{fl}}(T, \mathrm{lub})$ is the friction force, parallel to the conveyor belt and R_{P} stands for pulling chain sprocket pitch radius (see Fig. 14). For the details, see Appendix.

(2) The second dissipative contribution originates from the basic conveyor inlet end turn the design of which is accomplished with the aid of curved rolling surfaces. In this case both sliding and rolling friction occurs (Fig. 14). Because of the stated presumption of the load distribution between the chains it is clear that the support chains in this case are not significantly loaded.

The sliding friction occurs between the pulling chain's pin and bushing during the chain link inflection on the curved rolling surface and is caused by the chain axial force N_{P2}.

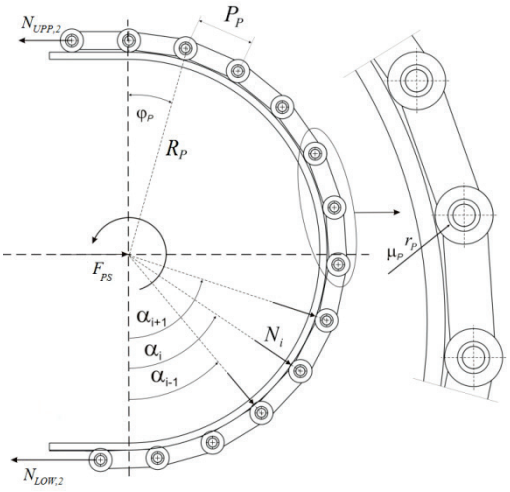

Figure 14 Geometry and forces during conveyor turn with the aid of rolling surfaces (inlet end of the basic design)

In addition to sliding friction due to link inflection also the friction due to rolling of the rollers of the strained pulling chain across the rolling surface is present. It consists of rolling friction of the rollers (of the radius r_{pr}) on rolling surface and sliding friction between the roller pin and roller bushing (of the radius r_{pb}). The magnitude of both friction contributions depend among others on the number of rollers in contact and on the value of normal force.

The required drive moment to overcome these effects is:

$$M_{f2} = R_P \cdot \left(F_{f2S} + F_{f2R}\right), \tag{5}$$

where F_{f2R} stands for total rolling and sliding friction contribution due to rolling of the rollers and F_{f2S} for sliding friction contribution due to the link inflection. For details, see Appendix.

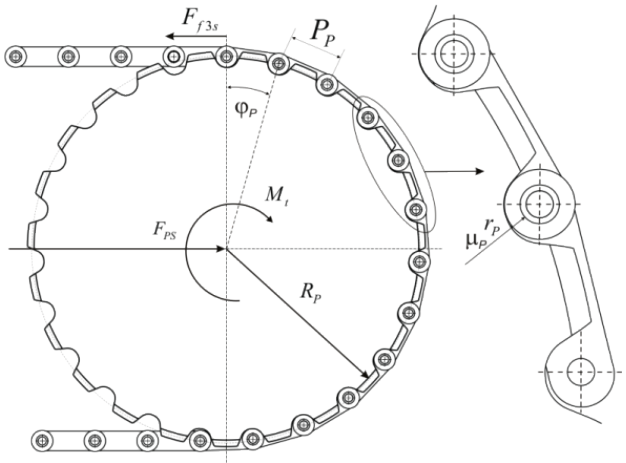

Figure 15 Geometry and forces during conveyor sprocket turn (inlet end of the second design and outlet end of both designs)

(3) Also where the conveyor turn is executed through sprocket wheels (Fig. 15) dissipative effects must be considered. Since there is almost no rolling friction due to sprocket design execution, only the pulling chain friction due to the link deflection must be considered using similar equation as before:

$$M_{f3} = R_P \cdot F_{f3}(T, \text{lub}), \tag{6}$$

where F_{f3} stands for sliding friction contribution due to the link inflection. For details, see Appendix.

To estimate the necessary drive power by analytical approach:

$$P_D^{An} = \omega_S \cdot M_f\,, \tag{7}$$

where ω_S is sprocket angular velocity, a total conveyor moment of resistance M_f must be defined:

$$M_f = \sum_i M_{f\,i} = R_P \cdot \sum_i F_{f\,i}\,, \tag{8}$$

from where the Eq. (7) can be rewritten as:

$$P_D^{An} = \omega_S \cdot R_P \cdot \sum_i F_{f\,i} = v \cdot \sum_i F_{f\,i}\,, \tag{9}$$

where v is conveyor velocity.

4.2 Equations for both conveyor designs

The first treated basic design is in this chapter denoted with additional index (1). It consists of sprocket chain turn at outlet side and the turn with the aid of curved rolling surfaces on the inlet side (Fig. 8). In this case all three friction sources, discussed in Chapter 4.1, are present, so power estimation Eq. (9) can be written as:

$$P_D^{An(1)} = v \cdot \left(F_{f1}^{(1)} + F_{f2}^{(1)} + F_{f3}^{(1)}\right), \tag{10}$$

where $F_{fi}^{(1)}$ is friction force of the i-th dissipative source of the first conveyor design. For details see Appendix.

The second conveyor design is denoted with additional index (2). It has a both sided sprocket turn execution (Fig. 9). In this case, the power estimation in the form of Eq. (9) is:

$$P_D^{An(2)} = v \cdot \left(F_{f1}^{(2)} + F_{f3-2}^{(2)} + F_{f3}^{(2)}\right), \tag{11}$$

where $F_{fi}^{(2)}$ is friction forces of the i-th dissipative source of the second conveyor design and where the source $i = 2$ (the basic inlet conveyor design) is replaced with $i = 3 \div 2$ (the sprocket wheel inlet conveyor design). For details see Appendix.

5 Results and discussions

The necessary driving power for both conveyor designs was calculated using equations introduced in Chapter 5 and the input data defined in Tab. 1.

Table 1 The input data

Sym.	Value/unit	Description
l	45 m	the length of the conveyor
r_{sr}	32,5 mm	radius of the support. chain roller
r_{pr}	32,5 mm	radius of the pulling chain roller
r_P	12,5 mm	pulling chain bushing radius
R_P	0,61 m	pull. chain sprocket pitch radius
P_P	160 mm	pulling chain pitch
i	180	driving gearbox gear ratio
v	0,5 m/s	max. conveyor velocity
f	0,5 mm	coefficient of rolling friction
μ_P	0,05 ÷ 0,06	sliding friction factor
$F_{g,\,mat}$	2100 kN	weight of transported material + process forces
$F_{g,\,con}$	321 kN	overall conveyor belt weight
F_{PS}	124 kN	force for straining the pull. chain

Friction resistance which results from conveyor and transported material weight and additional process forces which acts along the length of the conveyor is not dependant on the design case. Other friction contributions depend on conveyor turn execution.

To study the influences of separate factors on both of the conveyor designs the following cases have been observed.

In the first analysis the conveyor straining force is not present and the conveyor is not loaded (no material is transported). The determined friction contributions and required drive power for both conveyor designs are presented in Tabs. 2 and 3.

As expected, the main friction contribution comes from the conveyor own weight along the conveyor length (F_{f1}) since there are no other loading factors. In case of 1st conveyor design the friction contribution F_{f2}, which describes the dissipative effects in the area of curved rolling surfaces is present but its share is relatively small since there is no straining force considered. In both cases, the friction contribution F_{f3}, which describes the dissipative effects on the sprocket wheels, is present and negligible.

Table 2 Friction contributions and drive power for 1st conveyor design – no transported material, no chain straining

F_{f1} / kN	F_{f2} / kN	F_{f3} / kN	P_D^{An} / kW
9,85	0,80	0,01	1,07
92,5 %	7,46 %	0,08 %	

Table 3 Friction contributions and drive power for 2nd conveyor design – no transported material, no chain straining

F_{f1} / kN	F_{f3} / kN	P_D^{An} / kW
9,85	0,012	0,99
99,9 %	0,1 %	

It is obvious that the dissipative effects and the necessary driving power are smaller in the case of the second conveyor design.

In the second analysed case the chain straining forces are included into analysis whereas the load is still not considered. Friction resistance and drive power of both conveyor designs for described conditions are shown in Tabs. 4 and 5.

Table 4 Friction contributions and drive power for 1st conveyor design – no transported material

F_{f1} / kN	F_{f2} / kN	F_{f3} / kN	P_D^{An} / kW
9,86	20,9	0,20	3,09
31,8 %	67,6 %	0,6 %	

Table 5 Friction contributions and drive power for 2nd conveyor design – no transported material

F_{f1} / kN	F_{f3} / kN	P_D^{An} / kW
9,85	0,39	1,02
96,2 %	3,77 %	

From results shown it is evident that chain straining holds major influence on friction contribution F_{f2}. Its share raised from 7,46 % (0,80 kN) to 67,6 % (20,9 kN). Consecutively the 1st conveyor design drive power increases considerably from 1,07 kW to 3,09 kW (more than 200 % increase). For the 2nd conveyor design chain straining does not have much effect (only 3 % increase). For both designs the friction contribution on sprocket turn F_{f3} is negligible.

The final case which is presented in Tabs. 6 and 7, considers all loading factors. The chain straining force and transported material weight value used in calculation are evaluated according to real conditions in order to enable the comparison of analytically calculated and measured results. Because the precise value of friction coefficients μ_P and f are not known, the results are calculated for the diapasons from μ_P = 0,05 to 0,06 and f = 0,5 mm to 0,6 mm.

The drive power of both conveyor designs is proportional to sliding and rolling friction coefficients. It is evident that the sprocket turn is much more efficient and needs less driving power. The estimated difference is about 11 % in favour of the second design.

Table 6 Friction contributions and drive power for 1st conveyor design – all loadings included

	F_{f1} / kN	F_{f2} / kN	F_{f3} / kN	P_D^{An} / kW
μ_P = 0,05 f = 0,5 *mm*	77,54	10,26	0,11	8,79
	88,2 %	11,67 %	0,12 %	
μ_P = 0,055 f = 0,55 *mm*	85,29	11,96	0,13	9,74
	87,57 %	12,29 %	0,13 %	
μ_P = 0,06 f = 0,6 *mm*	93,05	13,81	0,15	10,7
	86,95 %	12,91 %	0,14 %	

Table 7 Friction contributions and drive power for 2nd conveyor design – all loadings included

	F_{f1} / kN	F_{f3} / kN	P_D^{An} / kW
μ_P = 0,05 f = 0,5 *mm*	77,54	0,15	7,77
	99,8 %	0,21 %	
μ_P = 0,055 f = 0,55 *mm*	85,29	0,18	8,55
	99,79 %	0,21 %	
μ_P = 0,06 f = 0,6 *mm*	93,05	0,2	9,32
	99,78 %	0,22 %	

When comparing the analytical and measured results we can see that the predicted savings of 11 % are reasonable close to the savings estimated by means of measurements. Also the absolute values of the calculated and measured dissipated power are comparable. For the first conveyor design the difference is (for considered

diapason of friction coefficients) between 8,5 % and 12 % and for the second conveyor design the difference is between 7 % and 12 %. The comparison shows that the analytical approach is precise enough to enable satisfactorily good prediction of the energy dissipation and it should be always used before the widely used design solutions are replaced with innovative designs.

6 Conclusion

Production of electric energy is directly related to CO_2 emissions. Since anthropogenic carbon dioxide concentration increase in earth atmosphere contributes directly to global warming, this is the point where the topic of energy consumption comes into play. That means that responsible and efficient energy consumption is the most important contributor to climate protection [9].

Comparison of two designs of the chain conveyor system for the curing chamber of the mineral wool insulation panels' production machinery was done after the measurement of the required driving power for both designs. The results show enhanced efficiency of the second design which reduced power consumption of the driving motor for 0,9 kW that presents 9 %.

Further, the analytical approach was used for the same task. The 11 % energy savings were predicted. The agreement of this result with measurements is satisfactory and therefore the analytical method is recommended to be used for energy efficiency analysis before the real-world implementation of the innovative designs.

Production machinery has built-in two identical conveyors and is intended to work 24 hours a day, approximately 340 days per year for about 20 years. For this reason the utilisation of the second design solution could bring savings of approximately 0,3 GW·h of electric energy.

Finally, the additional benefit in the environmental and cost reduction sense was detected during the operation. The quantity of the chain lubricant needed is in the case of the second design a few times lower than in the case of the first design.

Acknowledgement

This work has been supported by the Ministry of Education, Science, Culture and Sport of the Republic of Slovenia and by the Ministry of Education, Science and Technological Development of the Republic of Serbia under project 651-03-1251/2012-09/50 - The bilateral project for scientific cooperation between the Republic of Slovenia and the Republic of Serbia in the years 2012 - 2013.

The measurements were enabled by Knauf Insulation d.o.o., Škofja Loka, Slovenia.

7 References

[1] Kartnig, G.; Grösel, B.; Zrnić, N. Past, State-of-the-Art and Future of Intralogistics in Relation to Megatrends. // FME Transactions. 40, 4 (2012), pp. 193-200.

[2] Chains for power transmissions and material handling. // American Chain Association. New York: 1982.

[3] Broadfoot, A. R.; Betz, R.E. Prediction of power requirements for a longwall armored face conveyor. // IEEE Transactions on industry applications. 33, 1 (1997), pp. 80-89.

[4] Sloot, E. M.; Kruyt, N.P. Theoretical and experimental study of the transport of granular materials by inclined vibratory conveyors. // Elsevier, Powder Technology. 87, 3 (1996), pp. 203-210.

[5] Nayebi, A.; Mauvoisin, G.; Vaghefpour, H. Modeling of twist drills wear by a temperature-dependent friction law. // Journal of Materials Processing Technology. 207, 1-3(2008), pp. 98-106.

[6] Zrnić, N.; Rajković, M. Energy efficiency in intralogistics: A new trend in research. // Proceedings of the VII Triennial International Conference HEAVY MACHINERY - HM 2011. 7, 2(2011), pp. 127-132 / Vrnjačka Banja, Serbia, June 29th - July 1st, 2011.

[7] Humpl, D.; Starkl, F. The contributions of logistics to enhance energy efficiency in freight transport. // POMS 21st Annual Conference. / Vancouver, Canada, May 10, 2010.

[8] Günthner, W.; Tilke, Ch.; Rakitsch, S. Energy efficiency in bulk materials handling. // Bulk Solids Handling. 30, 3 (2010), pp. 138-142.

[9] Günthner, W.; Mirlach, M.; Rakitsch, S. Simulation of bulk materials ship unloading with a view to energy efficiency. // Bulk Solids Europe - Ship Unloading Energy Efficiency, 2010.

[10] Herrmann, C.; Mirlach, M.; Thiede, S. Process chain simulation to foster energy efficiency in manufacturing. // CIRP Journal of Manufacturing Science and Technology. 1, 4(2009), pp. 221-229.

[11] Duflou, JR.; Sutherland, JW.; Dornfeld, D; Herrmann, C; Jeswiet, J; Kara, S; Hauschild, M; Kellens, K. Towards energy and resource efficient manufacturing: A processes and systems approach. // CIRP Annals - Manufacturing Technology. 61, 2(2012), pp. 587-609.

Authors' addresses

Marko Langerholc, BSc
Knauf Insulation d.o.o.
Central Engineering Europe
Trata 3, 4220 Škofja Loka, Slovenija
marko.langerholc@knaufinsulation.com

Nenad Zrnić, Assoc. Prof., PhD
University of Belgrade
Faculty of Mechanical Engineering
80 Kraljice Marije Str.
11000 Belgrade, Serbia
nzrnic@mas.bg.ac.rs

Miloš Đorđević, BSc
University of Belgrade
Faculty of Mechanical Engineering
80 Kraljice Marije Str.
11000 Belgrade, Serbia
mddjordjevic@mas.bg.ac.rs

Boris Jerman, Assist. Prof., PhD
University of Ljubljana
Faculty of Mechanical Engineering
Aškerčeva cesta 6
SI-1000 Ljubljana, Slovenija
boris.jerman@fs.uni-lj.si

Appendix

In this chapter the details are given of the derivation of equations introduced in Chapter 4.

(1) The first dissipative contribution. The normal force on one supporting chain originating from conveyor own weight and integral weight of transported material (and possible production forces) is:

$$F_{\mathrm{N}} = 0{,}5 \cdot \left(\frac{F_{\mathrm{g,\,con}}}{2} + \frac{1}{l} \cdot \int_0^l F_{\mathrm{g,\,mat}}(x)\,\mathrm{d}x \right), \tag{12}$$

where $F_{\mathrm{g,\,con}}$ is overall conveyor weight (working and returning branch), and $F_{\mathrm{g,\,mat}}(x)$ stands for the distribution of the weight of the transported material along the conveyor length l. Using Eq. (12) the Eq. (3) can be rewritten considering both loads, double roller contact, and by assumption that in this case the sliding friction can be neglected:

$$F_{\mathrm{fl}}(T, lub) = 2 \cdot \frac{f}{r_{\mathrm{sr}}} \cdot F_{\mathrm{N}} = \frac{f}{r_{\mathrm{sr}}} \cdot \left(\frac{F_{\mathrm{g,\,con}}}{2} + F_{\mathrm{g,\,mat}} \right), \tag{13}$$

where r_{sr} stands for the support chain roller radius. The necessary drive moment to overcome this friction is defined in Eq. (4).

(2) The second dissipative contribution. The sliding friction occurs between the pulling chain's pin and bushing during chain link inflection and is caused by chain axial force N_{P2}:

$$M_{\mathrm{tr2}} = N_{\mathrm{P2}} \cdot \mu_{\mathrm{P}} \cdot r_{\mathrm{P}}, \tag{14}$$

Where r_{P} stands for pulling chain bushing radius (Fig. 13), and μ_{P} for sliding friction coefficient between pulling chain pin and bushing. The axial force in pulling chain N_{P2} depends on the angle α_i:

$$N_{\mathrm{P2}} = N_{\mathrm{LOW,\,2}} + \frac{\widehat{\alpha}_i}{\pi} \cdot \left(N_{\mathrm{UPP,\,2}} - N_{\mathrm{LOW,\,2}} \right), \tag{15}$$

and is:

$$N_{\mathrm{P2}} = N_{\mathrm{UPP,\,2}}, \tag{16}$$

for the upper side, where the chain is leaving the rolling surface and:

$$N_{\mathrm{P2}} = N_{\mathrm{LOW,\,2}}, \tag{17}$$

for the lower side, where the chain is coming onto the rolling surface.

One chain link will inflect for angle φ_{P} in the course of travelling the distance of two chain pitches P_{P} across the curved rolling surface and forming the angle twice the pitch angle φ_{P}, which is defined as:

$$\varphi_{\mathrm{P}} = 2 \cdot \arcsin\left(\frac{P_{\mathrm{P}}}{2 \cdot R_{\mathrm{P}}} \right). \tag{18}$$

The work required to inflect one chain link is therefore:

$$A_{\mathrm{tr,\,P},\,i} = M_{\mathrm{tr2}} \cdot 2\varphi_{\mathrm{P}} = \left(N_{\mathrm{P2}} \cdot \mu_{\mathrm{P}} \cdot r_{\mathrm{P}} \right) \cdot 2\varphi_{\mathrm{P}} = F_{\mathrm{f2S},\,i} \cdot 2P_{\mathrm{P}}, \tag{19}$$

where F_{f2S} stands for the pulling force required for one chain link inflection and can be expressed as:

$$F_{\mathrm{f2S},\,i} = \frac{N_{\mathrm{P2}} \cdot \mu_{\mathrm{P}} \cdot r_{\mathrm{P}} \cdot \varphi_{\mathrm{P}}}{P_{\mathrm{P}}}. \tag{20}$$

It has to be taken into account that two chain links deflect at the same time on the incoming lower side and two additional on the outgoing upper side:

$$F_{\mathrm{f2S}} = 2 \sum_{i=\mathrm{LOW}}^{\mathrm{UPP}} F_{\mathrm{f2S},\,i} = 2 \cdot \frac{\mu_{\mathrm{P}} \cdot r_{\mathrm{P}} \cdot \varphi_{\mathrm{P}}}{P_{\mathrm{P}}} \left(N_{\mathrm{LOW,\,2}} + N_{\mathrm{UPP,\,2}} \right). \tag{21}$$

In addition to the sliding friction due to link inflection also the friction due to rolling of the rollers of the strained pulling chain across the rolling surface is present. It consists of rolling friction of the rollers (of the radius r_{pr}) on rolling surface and sliding friction between the roller pin and roller bushing (of the radius r_{pb}). The magnitude of both friction contributions depends on the number of rollers in contact and on the value of normal force. For the i-th roller, a normal force is:

$$N_i = 2 \cdot N_{\mathrm{P2}} \cdot \sin\left(\frac{\varphi_{\mathrm{P}}}{2} \right), \tag{22}$$

where the N_{P2} is defined in Eq. (15).

Rolling friction of the i-th roller is:

$$F_{\mathrm{f2R}i} = N_i \cdot \frac{f}{r_{\mathrm{pr}}}. \tag{23}$$

Sliding friction for the i-th roller is defined through the equation for its moment of resistance:

$$M_{\mathrm{tr2S}i} = N_i \cdot \mu_{\mathrm{P}} \cdot r_{\mathrm{pb}} = F_{\mathrm{f2S}i} \cdot r_{\mathrm{pr}}, \tag{24}$$

where the same value of sliding friction factor is presumed as is used for chain pin. From Eq. (24) the i-th friction force is given as:

$$F_{\mathrm{f2S}i} = N_i \cdot \mu_{\mathrm{P}} \cdot \frac{r_{\mathrm{pb}}}{r_{\mathrm{pr}}}. \tag{25}$$

Total rolling and sliding friction contribution due to rolling of n rollers is:

$$F_{\mathrm{f2R}} = \sum_{i=1}^{n} \left(F_{\mathrm{f2R}i} + F_{\mathrm{f2S}i} \right). \tag{26}$$

The friction resistances due to the links inflection and due to rolling along the rolling surface are summed together:

$$F_{\mathrm{f2}}(T, \mathrm{lub}) = F_{\mathrm{f2S}} + F_{\mathrm{f2R}}, \tag{27}$$

and from there the corresponding drive moment required to overcome it, is defined (see Eq. (5)).

(3) The third dissipative contribution. Since there is almost no rolling friction, only the pulling chain friction due to the link deflection must be considered using similar equations as before (Eqs. (14) and (19)):

$$M_{\mathrm{tr3}} = N_{\mathrm{P3}} \cdot \mu_{\mathrm{P}} \cdot r_{\mathrm{P}}, \tag{28}$$

$$M_{\mathrm{tr3}} \cdot \varphi_{\mathrm{P}} = F_{\mathrm{f3S}} \cdot P_{\mathrm{P}}, \tag{29}$$

where axial force in the pulling chain is now denoted as N_{P3}. In analogy with Eqs. (20) and (21) the sliding and overall friction resistance F_{f3} can be expressed as:

$$F_{\mathrm{f3S},i} = \frac{N_{\mathrm{P3}} \cdot \mu_{\mathrm{P}} \cdot r_{\mathrm{P}} \cdot \varphi_{\mathrm{P}}}{P_{\mathrm{P}}}, \tag{30}$$

$$F_{\mathrm{f3}} = F_{\mathrm{f3S}} = 2 \sum_{i=\mathrm{LOW}}^{\mathrm{UPP}} F_{\mathrm{f3S},i} = 2 \frac{\mu_{\mathrm{P}} \cdot r_{\mathrm{P}} \cdot \varphi_{\mathrm{P}}}{P_{\mathrm{P}}} \left(N_{\mathrm{LOW,3}} + N_{\mathrm{UPP,3}} \right). \tag{31}$$

and in analogy with Eq. (5) the corresponding drive moment to overcome this contribution is defined in Eq. (6).

The friction forces from Eq. (10) for the first conveyor design. Friction force $F_{f1}^{(1)}$ can be derived in accordance with Eqs. (12) and (13).

Friction force $F_{\mathrm{f}\,2}^{(1)}$ on curved rolling surfaces is (in accordance with Eq. (27)) the sum of two contributions, where sliding friction contribution due to chain link inflection $F_{\mathrm{f}\,2,\mathrm{S}}^{(1)}$ is defined by Eq. (21). The rolling friction contribution $F_{\mathrm{f}\,2,\mathrm{R}}^{(1)}$ is defined in accordance with Eqs. (23), (25) and (26). The normal force N_i is further defined by Eqs. (22) and (15). The needed axial forces $N_{\mathrm{LOW,2}}$ and $N_{\mathrm{UPP,2}}$ are defined as:

$$N_{\mathrm{LOW,2}}^{(1)} = \frac{F_{\mathrm{PS}}}{4} + \frac{f}{r_{\mathrm{pr}}} \cdot \frac{F_{\mathrm{g,con}}}{4}, \tag{32}$$

where instead of double rolling contact on the supporting chain (as assumed in Eq. (13) for working branch) the conveyor is in the returning branch supported by pulling chain in single rolling contact, and:

$$N_{\mathrm{UPP,2}}^{(1)} = \frac{F_{\mathrm{PS}}}{4} + \frac{f}{r_{\mathrm{pr}}} \cdot \frac{F_{\mathrm{g,con}}}{4} + F_{\mathrm{f2}}^{(1)}. \tag{33}$$

Friction force during sprocket turn $F_{\mathrm{f}\,3}^{(1)}$ is defined by Eq. (31) where tension forces in upper and lower branch of the conveyor (Fig. 8) are:

$$N_{\mathrm{LOW,3}}^{(1)} = \frac{F_{\mathrm{PS}}}{4}, \tag{34}$$

$$N_{\mathrm{UPP,3}}^{(1)} = \frac{F_{\mathrm{PS}}}{4} + \frac{f}{r_{\mathrm{pr}}} \cdot \frac{F_{\mathrm{g,con}}}{4} + F_{\mathrm{f2}}^{(1)} + \frac{f}{r_{\mathrm{sr}}} \cdot \left(\frac{F_{\mathrm{g,con}}}{2} + F_{\mathrm{g,mat}} \right). \tag{35}$$

The friction forces $F_{\mathrm{f}\,i}^{(2)}$ from Eq. (11) for the second conveyor design (Fig. 9) are as follows. The friction force $F_{\mathrm{f}\,1}^{(2)} = F_{\mathrm{f}\,1}^{(1)}$ and force $F_{\mathrm{f}\,3}^{(2)}$ is derived, considering Eq. (31), where:

$$N_{\mathrm{UPP,3}}^{(2)} = \frac{F_{\mathrm{PS}}}{4} + \frac{f}{r_{\mathrm{pr}}} \cdot \frac{F_{\mathrm{g,con}}}{4} + F_{\mathrm{f3-2}}^{(2)} + \frac{f}{r_{\mathrm{sr}}} \cdot \left(\frac{F_{\mathrm{g,con}}}{2} + F_{\mathrm{g,mat}} \right), \tag{36}$$

and $N_{\mathrm{LOW,3}}^{(2)} = N_{\mathrm{LOW,3}}^{(1)}$. Also force $F_{\mathrm{f}\,3-2}^{(2)}$ is derived in accordance with Eq. (31), where $N_{\mathrm{LOW,3}}$ is replaced with $N_{\mathrm{LOW,2}}^{(2)} = N_{\mathrm{LOW,2}}^{(1)}$ and $N_{\mathrm{UPP,3}}$ with:

$$N_{\mathrm{UPP,2}}^{(2)} = \frac{F_{\mathrm{PS}}}{4} + \frac{f}{r_{\mathrm{pr}}} \cdot \frac{F_{\mathrm{g,con}}}{4} + F_{\mathrm{f3-2}}^{(2)}. \tag{37}$$